

UK/93-02

Origin of Difference Between \bar{d} and \bar{u} Partons in the Nucleon

Keh-Fei Liu and Shao-Jing Dong
 Department of Physics and Astronomy
 University of Kentucky
 Lexington, KY 40506

Abstract

Using the Euclidean path-integral formulation for the hadronic tensor, we show that the violation of the Gottfried sum rule does not come from the disconnected quark-loop insertion. Rather, it comes from the connected (quark line) insertion involving quarks propagating in the backward time direction. We demonstrate this by studying sum rules in terms of the scalar and axial-vector matrix elements in lattice gauge calculations. The effects of eliminating backward time propagation are presented.

PACS numbers: 13.60.Hb, 11.15.Ha, 12.38.Gc

A recent measurement of the Gottfried sum rule (GSR), defined in terms of the difference between the proton and neutron structure functions $F_2(x)$ in the integral $S_G = \int_0^1 dx [F_2^p(x) - F_2^n(x)]/x$, by the New Muon Collaboration (NMC) [1] has shown a disagreement with the expectation of the naive parton model. Assuming charge or isospin symmetry, the sum rule S_G can be expressed in terms of the parton distributions in the parton model as

$$S_G = \frac{1}{3} + \frac{2}{3} \int_0^1 dx [\bar{u}^p(x) - \bar{d}^p(x)]. \quad (1)$$

The naive parton model which assumes the isospin symmetry in the “sea”, i.e. $\bar{u}^p(x) = \bar{d}^p(x)$, leads to the prediction that $S_G = 1/3$ [2]. However, the NMC data, extrapolated to $x = 0$ and 1, leads to a value $S_G = 0.24 \pm 0.016$ which implies that $\bar{u}^p(x)$ and $\bar{d}^p(x)$ are not the same in the proton with the number of \bar{u}^p less than that of \bar{d}^p .

This has generated a good deal of theoretical interest. The apparent isospin asymmetry in the sea was envisioned by Field and Feynman [3] as due to the Pauli

exclusion principle and has been modeled [4] with the Sullivan process [5] which considers the meson cloud in the nucleon and the chiral-quark model [6].

In order to gain insight into the origin of this large \bar{d}/\bar{u} difference in the “sea”, we will examine the deep inelastic scattering in the Euclidean path integral formalism. The advantage of this formalism is that one can follow the quark line of propagation in the Euclidean time and separate out different contributions in terms of the connected and disconnected quark line insertions to facilitate the discussion.

The deep inelastic scattering of muon on nucleon involves the hadronic tensor of the current-current correlation function in the nucleon, i.e.

$W_{\mu\nu}(q^2, \nu) = \frac{1}{2M_N} \langle N | \int \frac{d^4x}{2\pi} e^{iq \cdot x} J_\mu(x) J_\nu(0) | N \rangle_{spin\ ave.}$. This forward Compton amplitude can be obtained by considering the ratio of the four-point function $\langle O_N(t) J_\mu(\vec{x}, t_1) J_\nu(0, t_2) O_N(0) \rangle$ and the two point function $\langle O_N(t - (t_1 - t_2)) O_N(0) \rangle$, where $O_N(t)$ is the interpolation field for the nucleon at Euclidean time t with zero momentum. For example, $O_N(t)$ can be taken to be the 3 quark fields with the nucleon quantum numbers, $O_N = \int d^3x \varepsilon^{abc} \Psi^{(u)a}(x) ((\Psi^{(u)b}(x))^T C \gamma_5 \Psi^{(d)c}(x))$ for the proton.

As both $t - t_1 \gg 1/\Delta M_N$ and $t_2 \gg 1/\Delta M_N$, where ΔM_N is the mass gap between the nucleon and the next excitation (i.e. the threshold of a nucleon and a pion in the p-wave), the intermediate state contribution in the four-point and two-point functions will be dominated by the nucleon with the Euclidean propagator $e^{-M_N(t - (t_1 - t_2))}$. Hence,

$$\begin{aligned} \widetilde{W}_{\mu\nu}(\vec{q}^2, \tau) &= \frac{\frac{1}{2M_N} \langle O(t) \int \frac{d^3x}{2\pi} e^{-i\vec{q} \cdot \vec{x}} J_\mu(\vec{x}, t_1) J_\nu(0, t_2) O(0) \rangle}{\langle O(t - \tau) O(0) \rangle} \bigg|_{\substack{t - t_1 \gg 1/\Delta M_N \\ t_2 \gg 1/\Delta M_N}} \\ &= \frac{\frac{f^2}{2M_N} e^{-M_N(t - t_1)} \langle N | \int \frac{d^3x}{2\pi} e^{-i\vec{q} \cdot \vec{x}} J_\mu(\vec{x}, t_1) J_\nu(0, t_2) | N \rangle e^{-M_N t_2}}{f^2 e^{-M_N(t - \tau)}} \\ &= \frac{1}{2M_N V} \langle N | \int \frac{d^3x}{2\pi} e^{-i\vec{q} \cdot \vec{x}} J_\mu(\vec{x}, t_1) J_\nu(0, t_2) | N \rangle, \end{aligned} \quad (2)$$

where $\tau = t_1 - t_2$, f is the transition matrix element $\langle 0 | O_N | N \rangle$, and V is the 3-volume. The hadronic tensor can be obtained formally by the inverse Laplace transform [7],

$$W_{\mu\nu}(q^2, \nu) = \frac{V}{i} \int_{c-i\infty}^{c+i\infty} d\tau e^{\nu\tau} \widetilde{W}_{\mu\nu}(\vec{q}^2, \tau) \text{ or through the integration } W_{\mu\nu}(q^2, \nu) = \frac{V}{4c} \lim_{\varepsilon \rightarrow 0} Re \int_0^c \varepsilon \tau^2 e^{(\nu + i\varepsilon)\tau} \widetilde{W}_{\mu\nu}(\vec{q}^2, \tau) d\tau \text{ with } c > 0.$$

In the Euclidean path-integral formulation, the four-point function can be classified into different groups depending on different topology of the quark paths between the source and the sink of the proton. They represent different ways the fields in the currents J_μ and J_ν contract with those in the nucleon interpolation operator O_N at different times. This is so because the quark action and the electromagnetic currents are both bilinear in quark fields, i.e. in the form of $\bar{\Psi} M \Psi$, so that the quark numbers are conserved and as a result the quark line does not branch the way a gluon line does. As illustrated in Fig. 1, we see Fig. 1(a) and 1(b) represent connected insertions (C.I.) where the quark fields from the currents contract with those from O_N

and the quark lines from $t = 0$ to $t = t$ are connected with the currents. Fig. 1(c), on the other hand, represents a disconnected insertion (D.I.) where the quark fields from J_μ and J_ν self-contract and are hence disconnected from the quark paths which originate from $O_N(0)$ and terminate at $O_N(t)$. Here, “disconnected” refers only to the quark lines. Of course, quarks sail in the background of the gauge field and all quark paths are ultimately connected through the gluon lines. The infinitely many possible gluon lines and additional quark loops are implicitly there in Fig. 1 but are not explicitly drawn. Fig. 1 represent the contributions of the class of “handbag” diagrams where the two currents are hooked on the same quark line. These are leading twist contributions in deep inelastic scattering. The other contractions involving the two currents hooking on different quark lines are represented in Fig. 2. Given a renormalization scale, these are higher twist contributions in the Bjorken limit. We shall neglect these “cat’s ears” diagrams in the following discussion.

In the deep inelastic limit where $x^2 \leq O(1/Q^2)$ (we are using the Minkowski notation here), the leading light-cone singularity of the current product (or commutator) gives rise to free quark propagator between the currents. In the time-ordered diagrams in Fig.1, Fig. 1(a)/1(b) involves only quark/antiquark propagator between the currents. Whereas, Fig. 1(c) has both quark and antiquark propagators. Hence, there are two distinct classes of diagrams where the antiquarks contribute. One comes from the D.I.; the other comes from the C.I.. It is frequently assumed that connected insertions involve only “valence” quarks which are responsible for the baryon number. But apparently, this is not true. To define the quark distribution functions more precisely, we shall call the antiquark distribution from the D.I., which are connected to the other quark lines through gluons, the *sea* antiquarks and the antiquarks from the C.I. the *cloud* antiquarks [8]. Thus, in the parton model, the antiquark distribution function can be written as

$$\bar{q}^i(x) = \bar{q}_c^i(x) + \bar{q}_s^i(x). \quad (3)$$

to indicate their respective origins in Fig. 1(b) and Fig. 1(c) for each flavor i . Similarly, the quark distribution will be written as

$$q^i(x) = q_V^i(x) + q_c^i(x) + q_s^i(x) \quad (4)$$

where $q_s^i(x)$ comes from Fig. 1(c) and both $q_V^i(x)$ and $q_c^i(x)$ come from Fig. 1(a). Since $q_s^i(x) = \bar{q}_s^i(x)$, we define $q_c^i(x) = \bar{q}_c^i(x)$ so that $q_V^i(x)$ will be responsible for the baryon number, i.e. $\int u_V(x)dx = \int [u(x) - \bar{u}(x)]dx = 2$ and $\int d_V(x)dx = \int [d(x) - \bar{d}(x)] = 1$ for the proton.

We shall first examine Fig. 1(c). After the integration of the Grassman fields Ψ and $\bar{\Psi}$, the path-integral for Fig. 1(c) can be written as the correlated part of

$$\int d[A] e^{-S_G} \text{Tr}[M^{-1}(t_2, t_1) \gamma_\nu M^{-1}(t_1, t_2) \gamma_\mu] \text{Tr}[M^{-1}(t, 0) \dots M^{-1}(t, 0) \dots M^{-1}(t, 0) \dots]. \quad (5)$$

where A is the gluon field, S_G the gluon action, and M is the quark matrix in the bilinear quark action $\bar{\Psi} M \Psi$. $M^{-1}(t_1, t_2)$ denotes the quark propagator from t_2 to t_1 .

Note in eq.(5), the trace is over the color-spin as well as the flavor indices. Since the quark loop involving the currents is separately traced from those quark propagators $M^{-1}(t, 0)$ whose trace reflects the quantum numbers of the proton, eq.(5) does not distinguish a loop with the u quark from that with the d quark at the flavor-symmetric limit, i.e. $m_u = m_d$. These are referred to as sea quarks and sea antiquarks in the naive parton model, since they are connected to those quark propagators which are sensitive to the hadron state through the gluon lines. These sea quarks can not give rise to the violation of the GSR, since $\bar{u}_s = \bar{d}_s$. The isospin breaking will give a small effect in the order of $(m_u - m_d)/M_c$ [9], where M_c is the constituent quark mass which reflects the confinement scale. Hence, the isospin symmetry breaking effect will be at the 1% level. It does not explain the violation of the GSR which is at $\sim 30\%$ level [1]. On the other hand, the quark propagators connecting the currents in Fig. 1(b) will show up in the same trace along with other quark propagators connecting the interpolation fields. Therefore, the cloud antiquarks are subjected to the Pauli exclusion as does the valence quarks and cloud quarks in Fig. 1(a) [10]. Consider the Fock space where a u quark line does the twisting in Fig. 1(b), the simplest Fock space would then be $uuu\bar{u}d$. With 3 u quarks, this Fock space configuration might be more Pauli suppressed than the corresponding Fock space of $uudd\bar{d}$ with 2 u quarks and 2 d quarks. We believe this is the reason for the large \bar{d}/\bar{u} difference in the nucleon as revealed by the NMC data. Consequently, neglecting the isospin symmetry breaking, the sum rule S_G can be written as

$$S_G = \frac{1}{3} + \frac{2}{3} \int_0^1 dx [\bar{u}_c(x) - \bar{d}_c(x)] \quad (6)$$

How do we substantiate this claim? Instead of evaluating the hadronic tensor directly which involves a four-point function, we shall study matrix elements with one current which can be obtained from three point functions. In the spirit of the operator product expansion and the parton model, matrix elements of the twist-2 operators in the form $\langle N | \bar{\Psi} \Gamma \Psi | N \rangle$ are the sum rules of the parton distribution functions. This can be viewed as $x^2 \rightarrow 0$ in the Bjorken limit, the two currents at t_1 and t_2 merge into one so that the connected insertion of one local operator will have both types of paths represented in Fig. 1(a) and Fig. 1(b). In fact, there have been indirect evidences of the presence of the cloud antiquarks in the previous study of three point functions in the quenched lattice QCD calculations, such as the ρ meson dominance in the pion electric form factor [11] and the negative neutron charge radius [12]. It has also been considered in association with large N_c and chiral perturbation theory [13]. To explicitly reveal the existence of the cloud antiquarks, we shall consider the scalar and axial-vector matrix elements in lattice calculation. The scalar current expanded in the plane-wave basis

$$\int d^3x \bar{\Psi} \Psi(x) = \int d^3k \frac{m}{E} \sum_s [b^\dagger(\vec{k}, s) b(\vec{k}, s) + d^\dagger(\vec{k}, s) d(\vec{k}, s)] \quad (7)$$

is a measure of the quark and antiquark number up to the factor m/E . Since the first moment of the structure function F_2 is not expressible in terms of the forward matrix element of a leading twist-2 operator, the scalar matrix element has been taken as a measure of the quark and antiquark number with m/E approximated by a constant [14, 15]. For the lattice calculation, we shall consider quark masses ranging from the charm to strange. In this case, we expect the dispersion of E will be considerably narrow so that m/E will be close to unity. To further decrease the dependence on m/E and other lattice corrections like the finite volume effect, scaling, and finite lattice renormalization, we shall consider ratios of matrix elements. Furthermore, since we have shown that the sea quarks from the D.I. can not give any significant contribution to the GSR, we shall concentrate on the C.I.. The first ratio we calculate is the isoscalar to isovector forward scalar matrix element or scalar charge of the proton with C.I.. In the parton model, it should be written according to eqs. (3) and (4) as

$$R_s = \frac{\langle p|\bar{u}u|p\rangle - \langle p|\bar{d}d|p\rangle}{\langle p|\bar{u}u|p\rangle + \langle p|\bar{d}d|p\rangle} \Big|_{C.I.} = \frac{1 + 2 \int dx [\bar{u}_c(x) - \bar{d}_c(x)]}{3 + 2 \int dx [\bar{u}_c(x) + \bar{d}_c(x)]} \quad (8)$$

In view of the fact that S_G shows $\int dx [\bar{u}_c - \bar{d}_c] < 0$ experimentally, we expect this ratio to be $\leq 1/3$. Our lattice results based on quenched $16^3 \times 24$ lattice with $\beta = 6$ for the Wilson κ ranging between 0.154 to 0.105 which correspond to strange and twice the charm masses are plotted in Fig. 3. For heavy quarks (i.e. $\kappa \geq 0.140$ or $m_q a \geq 0.31$ in Fig. 3), the ratio is $1/3$. This is to be expected because the cloud antiquarks which involves Z-graphs are suppressed for non-relativistic quarks by $O(p/m_q)$. For quarks lighter than $\kappa = 0.140$, we find that the ratio is in fact less than $1/3$. We take this to be the evidence of the cloud antiquarks in eq. (8). To verify the fact that this is indeed caused by the backward time propagators, we perform the following simulation. In the Wilson lattice action, the backward time hopping is prescribed by the term $-\kappa(1 - \gamma_4)U_4(x)\delta_{x,y-a_4}$. We shall amputate this term from the quark matrix in our calculation of the quark propagator. As a result, the quarks are limited to propagating forward in time and there will be no Z-graph and hence no cloud quarks and antiquarks. The Fock space is limited to 3 valence quarks. This is what the naive quark model is supposed to describe by design. In this case, the scalar current in eq. (7) and the ratio in eq. (8) involve only the valence quarks. To the extent the factor m/E can be approximated by a constant factor, the ratio R_s in eq. (8) should be $1/3$. The lattice results of truncating the backward time hopping for the light quarks with $\kappa = 0.148, 0.152$ and 0.154 are shown as the dots in Fig. 3 with errors less than the size of the dots. We see that they are indeed equal to $1/3$. This shows that the deviation of R_s from $1/3$ is caused by the cloud quarks and antiquarks. In retrospect, this can also be used to justify approximating m/E by a constant factor in eq. (8). We also find that the isovector scalar charge of the proton (the numerator in eq. (8)) for the forward propagating case is greater than the case with both forward and backward time propagation in our lattice results. For instance,

the isovector scalar charges for the forward propagating case are 1.07(1) and 1.01(1) for $\kappa = 0.154$ and 0.152. Yet, they are 0.73(15) and 0.85(5) respectively for the case with both forward and backward propagations. Assuming the m/E factor to be the same for these two cases and other things being equal, it implies that $\int dx[\bar{u}_c - \bar{d}_c] < 0$ which is consistent with the NMC result.

We have also examined the ratio of the isoscalar to isovector axial charge (C.I. only) of the proton. In the parton model, the ratio can be written as

$$R_A = \frac{\langle p|\bar{u}\gamma_3\gamma_5 u|p\rangle + \langle p|\bar{d}\gamma_3\gamma_5 d|p\rangle}{\langle p|\bar{u}\gamma_3\gamma_5 u|p\rangle - \langle p|\bar{d}\gamma_3\gamma_5 d|p\rangle} C.I. = \frac{g_A^1}{g_A^3} C.I. = \frac{\int dx[\Delta u(x) + \Delta d(x)]}{\int dx[\Delta u(x) - \Delta d(x)]} C.I. \quad (9)$$

where $\Delta u(\Delta d)$ is the quark spin content of the $u(d)$ quark and antiquark in the C.I. At the non-relativistic limit, g_A^3 is 5/3 and g_A^1 for the C.I. is 1 (the spin of the proton is entirely carried by the quarks in this case) [16]. Thus, the ratio should be 3/5 and we did find this ratio for the heavy quarks in Fig. 4. For lighter quarks, the ratio dips under 3/5. We interpret this to be due to the cloud quark and antiquark. Again when we dropped the backward time propagation for the quarks, we find that the ratio shown as the dots in Fig. 4 becomes 3/5 for lighter quarks as predicted by the quark model.

There are phenomenological consequences for the cloud quarks and antiquarks. The structure functions extracted from the DIS need to reflect the definitions of the quark and antiquark distributions in eqs. (4) and (3). Since strange and charm quarks come only from the sea in Fig. 1(c), it is natural to expect that $\bar{u}, \bar{d} > \bar{s}, \bar{c}$ since the \bar{u} and \bar{d} have both the sea and the cloud parts. The neutron-proton mass difference can be understood in terms of the isovector scalar charge [14] in eq. (8). The violation of the GSR has been modeled in terms of the Sullivan process [4] and the chiral quark model [6]. Although these models give the right picture in terms of the cloud antiquarks, there are inevitable drawbacks in the effective theories. For example, the Sullivan process where the photon couples to the antiquark in the meson as depicted in Fig. 5(a) can be drawn in terms of the quark lines in Fig. 5(b). However, Fig. 5(b) is only half of the story as far as the forward Compton amplitude is concerned. Upon attempting to complete the other half, one has a choice of taking the mirror image of Fig. 5(b) which will lead to the D.I. in Fig. 1(c) which does not contribute to the GSR. Alternatively, one could sew the quark lines with one of them twisted which will then lead to Fig. 1(b) and this does contribute to the GSR. The Sullivan process and the chiral quark model do not distinguish these two different topological possibilities.

In conclusion, we have shown in the Euclidean path-integral formalism that the experimentally observed \bar{d}/\bar{u} difference in the proton comes from the C.I. which involves cloud quarks and antiquarks. We have studied it in terms of the ratios of the isovector to isoscalar scalar and axial charges of the proton in the lattice calculations for the C.I.. We found that these ratios have the expected non-relativistic and relativistic limits as far as the cloud antiquarks are concerned. We demonstrate

this by truncating the quark backward time propagation which leads to the quark model predictions for these ratios without cloud antiquarks. Other phenomenological implications related to the cloud quarks and antiquarks and the quark model will be explored in the future.

This work is supported in part by the DOE grant DE-FG05-84ER40154. The authors would like to thank G.E. Brown, N. Christ, T. Draper, G. Garvey, R. Mawhinney, J.C. Peng, R. Perry, J.W. Qiu, M. Rho, W. Wilcox, and R.M. Woloshyn for discussions. They also thank S. Brodsky for pointing out that a classification similar to the C.I. and D.I. has been discussed in S. J. Brodsky and I. Schmidt, Phys. Rev. **D43**, 179 (1991).

References

- [1] New Muon Collaboration, P. Amaudruz et al., Phys. Rev. Lett. **66**, 2712 (1991).
- [2] K. Gottfried, Phys. Rev. Lett. **18**, 1174 (1967).
- [3] R.D. Field and R.P. Feynman, Phys. Rev. D **15**, 2590 (1977).
- [4] S. Kumano, Phys. Rev. D **43**, 59, 3067 (1991); E.M. Henley and G.A. Miller, Phys. Lett. **B251**, 453 (1990); A. Siganl, A.W. Schreiber, and A.W. Thomas, Mod. Phys. Lett. **A6**, 271 (1991); W-Y. P. Hwang, J. Speth, and G.E. Brown, Z. Phys. **A339**, 383 (1991).
- [5] J.D. Sullivan, Phys. Rev. **D5**, 1732 (1972).
- [6] E. Eichten, I. Hinchliffe, and C. Quigg, Phys. Rev. **D45**, 2269 (1992).
- [7] W. Wilcox, Nucl. Phys. **B**(Proceedings of Lattice 92, Amsterdam, Sept. 1992), to be published.
- [8] As will be shown elsewhere, these anti-quarks are related to the meson clouds in those hadronic models which incorporate the flavor non-singlet meson cloud picture in the structure.
- [9] D.J. Gross, S.B. Treiman, and F. Wilczek, Phys. Rev. **D19**, 2188 (1979).
- [10] To state it in another way, any Pauli exchange diagram between the sea quark/antiquark and those quarks/antiquarks connecting the interpolating fields in Fig. 1(c) will inevitably end up in the C.I. in Fig. 1(a) or Fig. 1(b). Whereas, the Pauli exchange diagrams of the C.I. insertion can still be in the class of the C.I..
- [11] T. Draper, R.M. Woloshyn, K.F. Liu, and W. Wilcox, Nucl. Phys. **B318**, 319 (1989).

- [12] W. Wilcox, T. Draper, and K.F. Liu, Phys. Rev. **D46**, 1109 (1992).
- [13] T. Cohen and D.B. Leinweber, U. of Md. PP #92-189; S. Sharpe, Phys. Rev. **D41**, 3233 (1990); C. Bernard and M. Golterman, Phys. Rev. **D46**, 853 (1992).
- [14] S. Forte, Phys. Rev. **D47**, 1842 (1993).
- [15] S. Weinberg, *A Festschrift for I.I. Rabi*, ed. L. Motz (N.Y. Academy of Sciences, NY, 1977); J. Gasser and H. Leutwyler, Phys. Rep. **87**, 77 (1982).
- [16] K.F. Liu, Phys. Lett. **B281**, 141 (1992).

Figure Captions

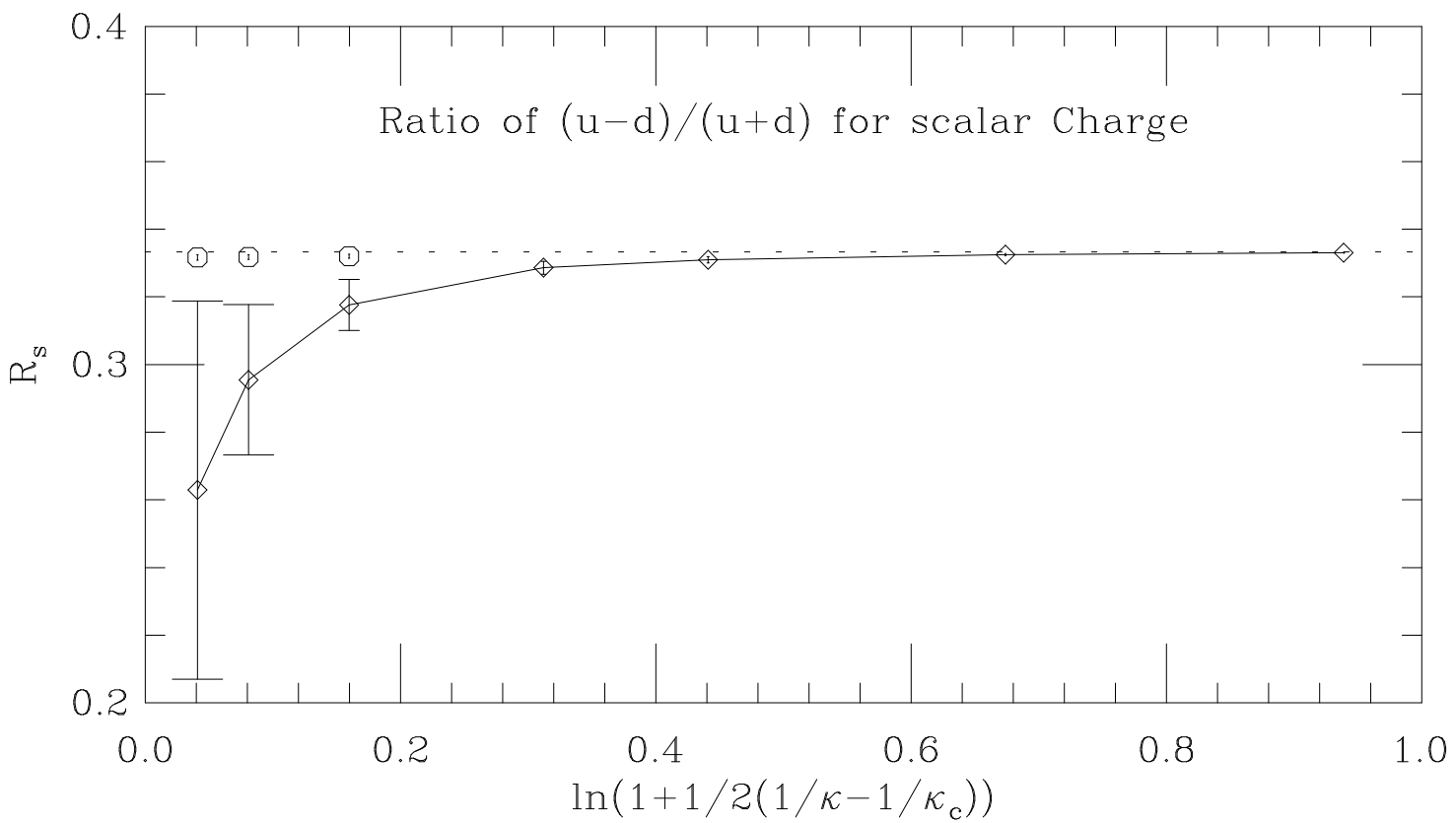
Fig. 1 Time-ordered “handbag” skeleton diagrams of quark lines with different topologies. (a)/(b) is the C.I. involving a quark/antiquark propagator between the currents. (c) is a D.I. involving sea quarks and antiquarks.

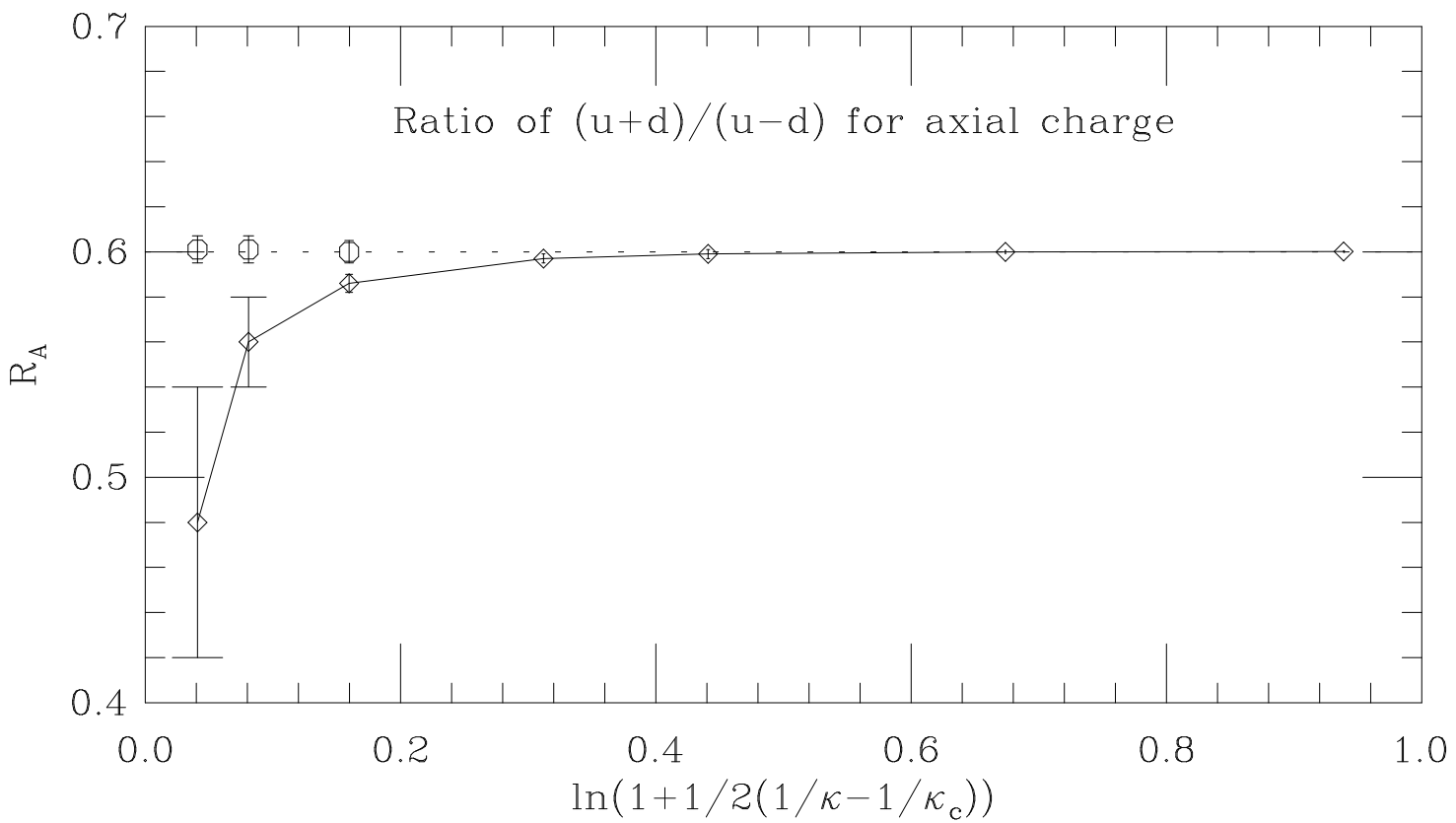
Fig.2 Cat’s ears diagrams.

Fig. 3 The ratio of the isovector to isoscalar scalar charge of the proton for the C.I. (shown as \diamond) is plotted as a function of the quark mass m_q in the lattice unit a . The errors are obtained from the jackknife method. The errors of the dots are smaller than the size of the dots.

Fig. 4 The ratio of the isoscalar to isovector g_A of the proton for the C.I. as a function of the quark mass.

Fig. 5 (a) Sullivan process in terms of the meson and baryon lines. (b) The same process drawn in terms of the quark lines.





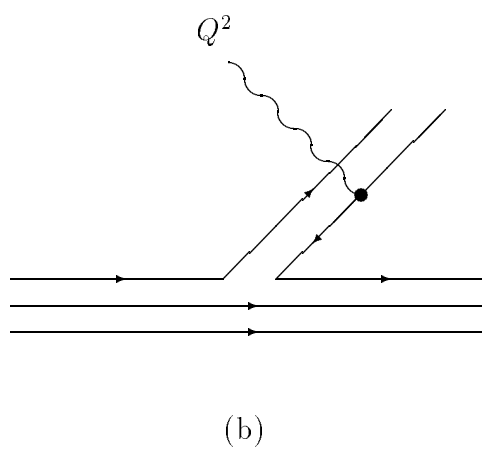
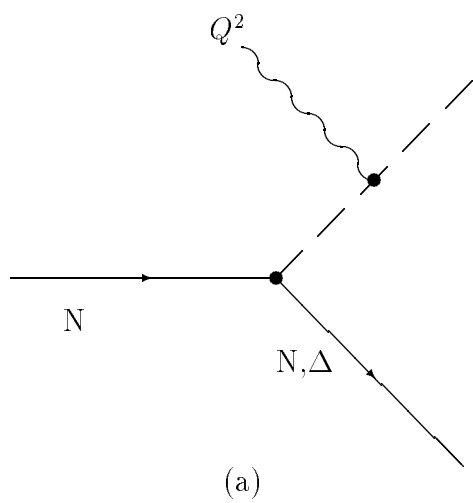


Fig.5

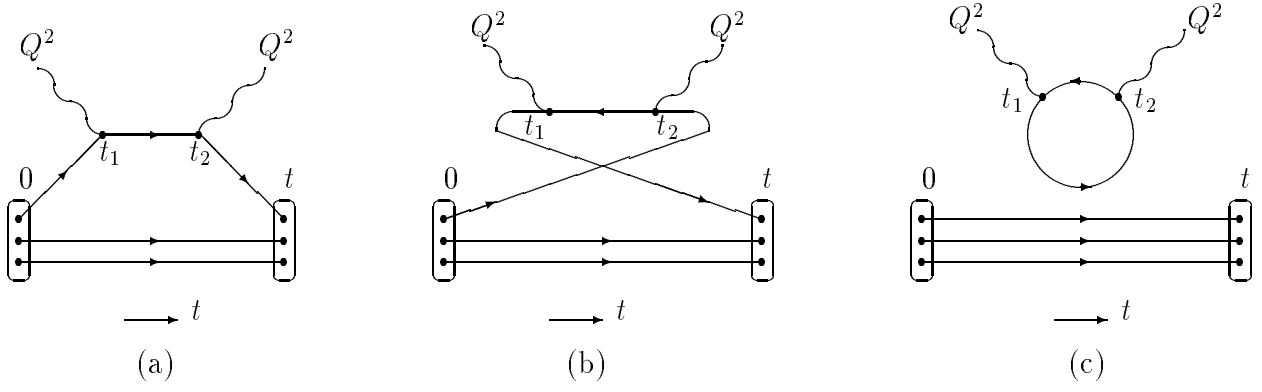


Fig.1

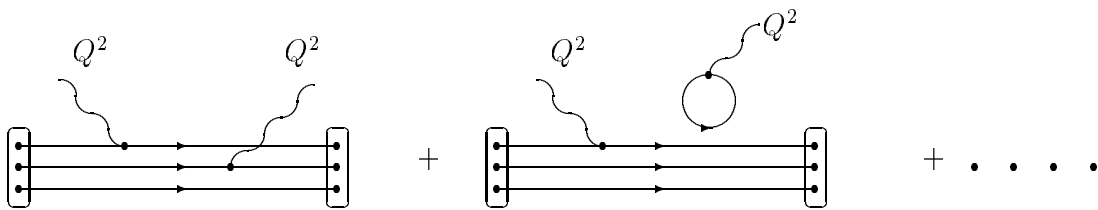


Fig.2